Proceedings of the 11th Brazilian Congress of Thermal Sciences and Engineering -- ENCIT 2006
Braz. Soc. of Mechanical Sciences and Engineering -- ABCM, Curitiba, Brazil,- Dec. 5-8, 2006

Paper CIT06-1060

Thermal Performance of Nuclear Fuel Rods with a Jacobian Elliptic Cross Sectional Form

De Aguiar, João B.
Sistemas Mecânicos, Escola Politécnica, USP
Av. Prof. Mello Moraes, 2231, São Paulo, SP, 05508-900
jbaguiar@usp.br
Tu, Carlos C.C., Abe, Luciano
Sistemas Mecânicos Escola Politécnica, USP
carlcctu@usp.br; Luciano.abe@poli.usp.br

Abstract. Boiling water reactors, BWR, commercially use fuel rods with a circular cross section. Set the operational conditions as well as the distribution of these rods, a specific power is established. Changing this form while conserving the cross sectional area may deliver a better performance. This fact is investigated here for a family of elliptic forms, in a thermal sense, using the finite element method. Two limiting values are considered: the melting temperature of the fuel and the critical flux rate. For 2d models, gains of the order of twenty percent in performance are estimated. It is also perceived the advantage of this alteration in other form of reactor, and discussed means of addressing other aspects of the problem.

Keywords: elliptic fuel rod; temperature field; power performance, finite element

1. Presentation

Commercial nuclear reactors use fuel rods of uranium oxide, UO_2, of circular cross section, followed by a gap filled with nuclear combustion gases, helium mostly, and protected by cladding material, responsible for the final heat exchange with the cooling fluid, the water. These rods are distributed in many bundles, arranged in a regular form, inside the core of the reactor. Once initiated the nuclear activity in the reactor, water in liquid phase enters at prescribed temperature and pressure, flows along the length of the rods, leaving in a boiling state (Glasstone & Sesonski, 1994) Maximum temperature position in each rod, as well as heat flow lines set the field for circular rods. And consequently its specific power capacity. However in peak demand it is important to be able to get some additional power output, reason why a different form of cross sectional geometry for the rods, hence with different thermal fields, is devised.

Here a family of forms is proposed, having the same cross sectional area of commercial circular rods. Finite element modeling is used to obtain the temperature and heat flux field, in a two-dimensional case, observing the same physical restrictions of maximum temperature and critical heat flux, section 2. Under the typical operating conditions of a BWR, section 3, the physical limits are evaluated and the numerical procedure discussed. Results are presented in section 4 for diverse forms and, in particular, the circular form is checked, for the accuracy of the discretized solution. Analytical results for this case are also restated. Characteristics of better forms are analyzed then.

2. Model

2.1 Geometry

Proposed new format for the transversal sectional forms of the fuel rods, Fig. 1, will derive from a family of curves defined from elliptic jacobian functions (Milne-Thomson, L.M.,1950) resultant from the transform:

$$\bar{z} = a\, cn(w); \quad \bar{z} = x - iy \quad w = u + iv \tag{1}$$

between the w-plane and the z-plane. From the addition formula of the cn function, geometric locus in the $< x, y >$ plane for every equipotential $v = v_0$ value at different settings of parameter m, is:

$$x = a\frac{cn(u/m)cn(v/1-m)}{cn^2(v/1-m)+msn^2(u/m)sn^2(v/1-m)}$$
$$y = a\frac{sn(u/m)dn(u/m)sn(v/1-m)dn(v/1-m)}{cn^2(v/m)+msn^2(u/m)sn^2(v/1-m)} \quad (2)$$

where the elliptic functions cn and dn:

$$cn(u,v/m) = \sqrt[2]{1-sn^2(u,v/m)}$$
$$dn(u,v/m) = \sqrt[2]{1-msn^2(u,v/m)} \quad (3)$$

derive, for every u or v, at each value of m from the sn function, defined according to the integral:

$$sn^{-1}(u,v/m) = \int_0^{u,v} \frac{dt}{\sqrt{(1-t^2)(1-mt^2)}} \quad (4)$$

This function is known as Jacobian elliptic function. It is a Legendre elliptic integral of the first kind.

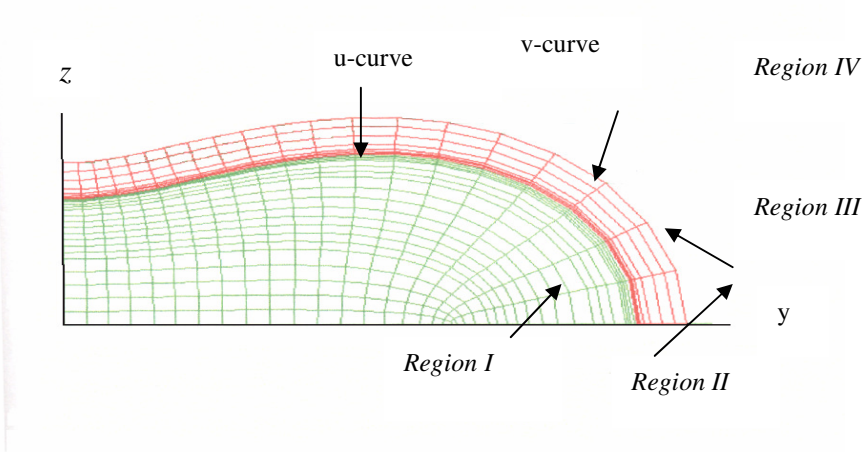

Fig. 1 Element of the family of new forms showing the diverse regions of the problem

A part this geometric form, the common circular rod of radius a:

$$< x, y > / \quad y = \sqrt{a^2 - x^2} \quad (5)$$

that can also be represented in integral form from $y = \int_0^x \frac{-t}{\sqrt{a^2-t^2}} dt$, in the first quadrant, will be used as a comparison form for evaluation of the new format.

2.2 Energy Equation

Local rate form of the energy equation relates the rate of variation of the internal energy to the rate of external work and heat exchange:

$$\rho\dot{\mu} = -\boldsymbol{\sigma} : \mathbf{D} + Div\mathbf{q} + q_b; \quad Div = Grad \cdot \tag{6}$$

Here the internal energy per unit volume μ is a function of the point and temperature θ $\mu = \hat{\mu}(.,\theta)$, ρ stands for the mass density, $\mathbf{q}$ is the heat flux vector, supposed independent of strains or displacements, $\mathbf{q} = \hat{\mathbf{q}}(.,\theta)$ and q_b represents the internal heat generation rate, obtained from the solution of the neutron diffusion problem, (Winterton, R.H.S.,1981)

For the plane problem, unit thickness, under permanent conditions while disregarding coupling caused by the work term $\boldsymbol{\sigma} : \mathbf{D}$, being $\boldsymbol{\sigma}$ the stresses and $\mathbf{D}$ the deformation gradient rate, in integral form:

$$\int_S \mathbf{q}.\mathbf{n}dA + \int_V q_b dV = 0 \tag{7}$$

Here latent heat effects and phase changes are disregarded. Surfaces S include temperature specified surfaces S_θ as well as flux specified surfaces S_q.

As a general arrangement, fuel rods comprise an inner region, region 1, surrounded by an almost empty space, region 2, followed by a protection cladding, region 3, in contact with the cooling fluid, region 4. Fuel rod is made up of uranium oxide, UO_2, material 1, which is separated from the protection material, in our case Zircaloy, material 3, by means of gases resulting from nuclear reactions. These gases are mostly helium but also criptonium and xenonium, depending on the reactor considered, occur, material 2. For the first body, symmetry boundary conditions as well as continuity in the first interface impose that:

$$\begin{aligned} &\mathbf{q} = \mathbf{0}; \quad 0 \le y \le {}_1y \quad \wedge \quad 0 \le z \le {}_1z \\ &{}_1\mathbf{k} \cdot \frac{\partial\theta}{\partial\mathbf{n}} = {}_1q_2^n \quad on \quad {}_1S_2 \end{aligned} \tag{8}$$

being $\mathbf{k} = \hat{\mathbf{k}}(\theta)$ the matrix of thermal conductivity, term of Fourier's law. In the intermediate sector, as passage region, net flow is null:

$$\begin{aligned} &\int_{{}_1S_2+{}_2S_3} \mathbf{q} \cdot \mathbf{n}dA = 0; \\ &\mathbf{q} = \mathbf{0}; \quad {}_1y \le y \le {}_2y \quad \wedge \quad {}_1z \le z \le {}_2z \end{aligned} \tag{9}$$

where the horizontal y and vertical z limits for the $S_{q=0}$ surface, symmetry, have been established.

As there is no generation in the outer region, $\int_{{}_2S_3+{}_3S_4} \mathbf{q} \cdot \mathbf{n}dA = 0$ and $\mathbf{q} = \mathbf{0}$ for ${}_2y \le y \le {}_3y \quad \wedge \quad {}_2z \le z \le {}_3z$.

For the outer interface, ${}_3\mathbf{k} \cdot \frac{\partial\theta}{\partial\mathbf{n}} = {}_3q_4^n$ on ${}_3S_4$ where ${}_3q_4^n = q_t + q_c + q_r$ being:

$$\begin{aligned} &q_t = -\mathbf{k} \cdot Grad\theta; \quad Grad = \frac{\partial}{\partial\mathbf{X}}; \quad \mathbf{X}^T = \lfloor X, Y, Z \rfloor \\ &q_r = A(\theta^4 - \theta_r^4) = r(\theta - \theta_\infty^r) \\ &q_c = h(\theta - \theta_\infty^c) \end{aligned} \tag{10}$$

Of the diverse components of heat transfer, thermal conductivity q_t dominates, mostly in the core region. It is function of the conductivity matrix $\mathbf{k}$, supposed isotropic and dependent upon temperature. It is followed

in importance, by the convection heat transfer q_c for the interaction with the refrigerant, function of the conduction coefficient h_c and reference temperature in the fluid cell θ_∞^c. Also the radiation component q_r appears, which involves direction and form coefficient A in addition to the reference temperature θ_∞^r.

2.3 Principle of Virtual Temperatures

The principle of virtual temperatures (Bathe, K.J.,1995), which is a variational statement of energy balance, may be obtained directly by the standard Galerkin approach. Applied to the problem at hand, entails us to write:

$$\int_V Grad\delta\theta \cdot \mathbf{q} dV - \int_V \delta\theta \, q_b dV = \int_S \delta\theta \mathbf{q} \cdot \hat{\mathbf{n}} dS = 0 \tag{11}$$

where $\delta\theta$ is an arbitrary variational field satisfying the essential boundary conditions. In order to solve for the $\boldsymbol{\theta}$ field, the body is approximated geometrically with finite elements, so that the temperature is interpolated as:

$$\boldsymbol{\theta} = \mathbf{N}^N \boldsymbol{\theta}^N \tag{12}$$

being $\theta^{\mathbf{N}}$ the nodal temperatures. The Galerkin approach assumes that the variational field is interpolated by the same function. With these interpolations, the variational statement produces the system of equations:

$$\begin{aligned} &\mathbf{F}^N = \mathbf{0} \\ &\mathbf{F}^N = \int_S \mathbf{N}^N \cdot \mathbf{q} dS - \int_V Grad\mathbf{N}^N \cdot \mathbf{q} dV - \int_V \mathbf{N}^N q_b dV \end{aligned} \tag{13}$$

that can be solved for the nodal temperatures, if a Newton type of solutions is employed. Allowing for the diverse surface forms of heat transfer, Eq. (10), it leads to:

$$(\mathbf{K}_t + \mathbf{K}_c + \mathbf{K}_r)\boldsymbol{\theta} = \mathbf{Q}_b + \mathbf{Q}_r + \mathbf{Q}_c \tag{14}$$

where the matrices of conduction, convection and radiation are defined as:

$$\begin{aligned} &\mathbf{K}_t = \int_V \mathbf{B}^{NT} \mathbf{k} \mathbf{B}^N dV; \quad \mathbf{B} = Grad\mathbf{N}^N; \quad V = V_1 + V_2 + V_3 \\ &\mathbf{K}_c = \int_{S^c} \mathbf{N}^N \mathbf{h} \mathbf{N} dS; \quad S^c = {}_1S_2 + {}_2S_3 + {}_3S_4 \\ &\mathbf{K}_r = \int_{S^r} \mathbf{N}^N \mathbf{r} \mathbf{N}^N dS \end{aligned} \tag{15}$$

with no conductivity contact surface. The source terms are:

$$\mathbf{Q}_c = \int_{S^c} \mathbf{N}^N \mathbf{h} \theta_\infty^c dS \tag{16a}$$

$$\mathbf{Q}_r = \int_{S^r} \mathbf{N}^N r\theta_\infty^r dS \tag{16b}$$

$$\mathbf{Q}_b = \int_V \mathbf{N}^N q_b dV \tag{16c}$$

where S^c, S^r are convection and radiation surfaces. Furthermore, with diverse bodies, boundary and continuity conditions, will add the corresponding matrices in Eq. (14).

2.4 Physical Limits

In order to determine the real temperature field, Eq. (14), in the discretized problem, the free parameter q_b has to be set at every iteration of the solution process. Two physical limits have to be observed however. The first relates to an upper value of the temperature field, $\theta_u = \theta_{melting}$ of the core material. The other is related to the maximum allowable heat flow rate ${}_3q_4^n$, the critical flow rate to the surrounding water, $q_{critical.}$

3. Model Parameters

3.1 Input Values

A series of geometric forms were considered in the analysis. Forms depend upon the pair of parameters v and m .For both the set of values $< 0.2; 0.4; 0.5; 0.6; 0.7; 0.8 >$ was taken in a one-to-one combination. In every case the same cross sectional area of the circular element, $D = 11.4 \quad mm; \quad A = \pi D^2/4$ was imposed. Once set the cross sectional form of the fuel element, a gap f of values in the interval $0.25 \le f \le 0.73$ mm was taken. External cladding, following the same contour had value $c = 0.81$ mm. In some constructions no gap was considered. In others an external protection layer wasn't present as well.

Some thermal material properties are shown in table 1, for the representative values in the range encountered in the problem. In particular the coefficient of conductivity of the fuel, assumed isotropic, depends on temperatures. For it an approximate relation for the dependency in W/cm ^{0}C is:

$$k(\theta) = \frac{40.4}{464 + \theta} + 0.132e-03 \exp(0.00188\theta); \quad {}^0C \tag{17}$$

Table 1 Some physical properties of the materials

	$\rho\ [kg/mm^3]$	$k_t\ [W/mm\,{}^0C]$	$C_p\ [mJ/kg\,{}^0K]$
Uraninum oxide	10.980e-06	2.60e-03	0.31
Helium	0.0973e-09	0.211e-03	5.20
Zircaloy	6.5600e-06	16.5e-03	0.33

Coefficients of convection in the outer interface also depend upon local temperature. A range of variation exists, $4.0e-03 \le h_c \le 6.0e-03$ W/^{0} Kin the interval $285 \le \theta_c \le 350$ ^{0}C.

3.2 Numerical Scheme

In order to apply the linear thermal procedure associated with the finite element discretization, a Newton-Raphson scheme for the iterations has to devise. For every value of the free parameter $q_b{}^{(n)}$, corresponding to iteration n, and fixed the solid-fluid interaction parameters, a temperature field $\boldsymbol{\theta}^{(n)}$ may be obtained. For this solution however, in general, there is an unbalance of the vector $\mathbf{F}^{(n)}$, Eq. (13), that has to be dealt with. If it is assumed that in the next iteration, an increment of the heat generation rate Δq_b will be set so as to clear this unbalance, $\mathbf{F}^{n+1} = \mathbf{0}$, then:

$$\Delta q_b = -\frac{\mathbf{F}}{\partial_{,q_b}\mathbf{F}}\rangle_n \tag{17}$$

in a forward fashion. Evidently this increment, and the solution derived from it, has to satisfy the physical limits imposed to the problem. Moreover, as a one term expansion only is under consideration, care must be taken in the setting of an error value, for closure of the procedure. The initial trial point may be taken directly from the solution of the circular rod case. This has conducted, in general, to a few iterations.

The iterative scheme to be employed may be best described from the incremental form of Eq. (13):

$$\partial\mathbf{F} = \int_S \mathbf{N}^N \cdot \partial\mathbf{q}\, dS - \int_V Grad\mathbf{N}^N \cdot \partial[\mathbf{k}\frac{\partial\theta}{\partial\mathbf{X}}]dV - \int_V \mathbf{N}^N \partial q_b dV \tag{18}$$

where:

$$\partial\mathbf{q} = \partial\mathbf{k}\frac{\partial\theta}{\partial\mathbf{X}} + \mathbf{k}\frac{\partial}{\partial\mathbf{X}}\partial\theta + \partial q_c \mathbf{n}_c + \partial q_r \mathbf{n}_r \tag{19}$$

being $\mathbf{n}_c$ and $\mathbf{n}_r$ normal unit vector in the S_c and S_r partitions of the heat transfer S surface. Introducing Taylor expansions to the first order of the expressions above, in a Euler forward manner, the incremented form of $\mathbf{F}$ will be such that:

$$\begin{aligned} lhs &= \int_V \mathbf{B}^T \cdot \mathbf{k}\frac{\partial}{\partial\mathbf{X}}\partial\theta dV + \int_{S_c} \mathbf{N}^N h\partial\theta dS + \int_{S_r} \mathbf{N}^N r\partial\theta dS \\ rhs &= \int_{S_c} \mathbf{N}^N h[(\theta_c + \partial\theta_c) - \theta]dS + \int_{S_r} \mathbf{N}^N r[(\theta_r + \partial\theta_r) - \theta_r]dS + \int_V \mathbf{N}^N [q_b + \partial q_b]dV + \int_V \mathbf{B}\cdot\mathbf{k}\frac{\partial\theta}{\partial\mathbf{X}}dV \end{aligned} \tag{20}$$

where $lhs = rhs$. Referring the known quantities to iteration i, and the unknown quantities to iteration $i+1$, Eq. (20) can be rewritten as:

$$[\mathbf{K}_t^i + \mathbf{K}_c^i + \mathbf{K}_r^i]\partial\boldsymbol{\theta} + [\mathbf{K}_c^i + \mathbf{K}_r^i]\boldsymbol{\theta}^i = \mathbf{Q}_b^{i+1} + \mathbf{K}_c^i\boldsymbol{\theta}_c^{i+1} + \mathbf{K}_r^{i+1}\boldsymbol{\theta}_r^{i+1} \tag{21}$$

where $\boldsymbol{\theta}_c^{i+1}$ and $\boldsymbol{\theta}_r^{i+1}$ are the updated external convection/radiation fields. $\mathbf{Q}_b^{i+1}$ refers to the incremented body generation heat vector.

3.3 Physical Limits

Determination of the critical heat flux rate at the outer surface of the fuel rod requires coupling to the water flow problem, or use of some experimental formula. Though developed for BWR reactors and circular rods, Biasi formula may be used for the present case:

$$q_{crit} = 15.048e+7(100D)^{-n} G^{-0.6} H(1-x) \tag{22}$$

where:

$$H = -1.159 + 0.149p\exp(-0.019p) + 9p/(10+p^2) \tag{23}$$

for pressures p expressed in bars, and fraction:

$$x = \frac{q_{crit}}{\dot{m}h_{fg}} - \frac{\Delta h_{sub}}{h_{fg}} \tag{24}$$

with $\Delta h_{fg} = 0.398e+06$ J/kg and $h_{fg} = 1.51e+06$ J/kg. Typical reactor conditions were assumed: $p = 70$ bar; $\theta_{in} = 204\,^0$C, $G = 2.e+03$ kg/m^{2}s. A rectangular arrangement of the bundle of rods supposes a center to center distance $l = 18.82$ mm, used in finding the hydraulic diameter to be used above. Rods had an height of 3.2 m, Fig. 2.

The other limit, the melting point of the fuel rod, set at $\theta_{melting} = 2800\,^0$C. In the model running, temperature at the surface of the cladding shell was fixed at ${}_3\theta_4^s = 300\ ^0$C.

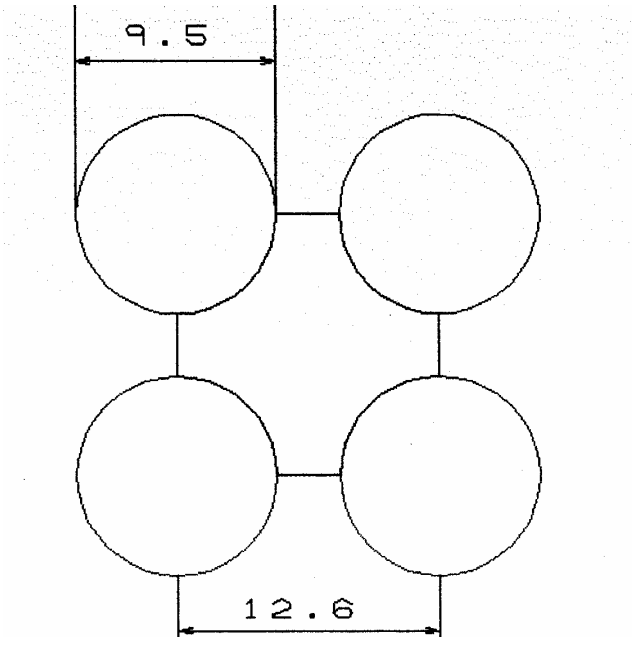

Fig.2 Typical cell distribution of fuel rods

4 Results

4.1 General Response

Implementation of the above scheme of solution for the different sectional forms led to a series of temperature and flux fields. Discretization involved different elements and densities, according to the region,
and some times added to more than a thousand elements. Maximum temperature and critical heat flow limits have been used in determining the solutions.
In Figs. 2 and 3, as an example, temperature and heat flux fields in the case of the elliptic form characterized by the $<0.7;0.5>$ pair is shown. In it surface temperature at the outer cladding is fixed.. Maximum temperature obtained, in the core region, is close to the maximum allowable, $\theta_u = 2800^0 C$, and appears in the central region of the rod. Many times maximum temperature will not occur at the origin. Moreover, flux values vary along the outer surface of the cladding, being larger in the points of the surface closer to the center of the rod.

As the response of the rod should change, if the slice being taken is changed along the length of the rod, because the internal heat generation rate, as well as the heat transfer limit, the most critical combination was considered. Position of maximum heat generation, in general occurs at middle length of the rod. Heat flow to the water, initially in liquid state, changes along the length of the rod, passing to a two phase flow and a final boiling condition. Convection coefficient, as such, changes as well. Formally this coefficient could be obtained experimentally and numerically. In the last case a fluid flow analysis would have to be run, so as to generate the velocities gradients, in a 3D model. Therefore setting , in the 2D model, the external surface is an approximation. The chosen temperature compares well with simulations and measures reported in the literature, and was therefore used in some analysis. Moreover, critical heat flux limits, used for the new forms, in the same amount as in the case of the circular rod, is another sort of approximation, used as an initial estimate.

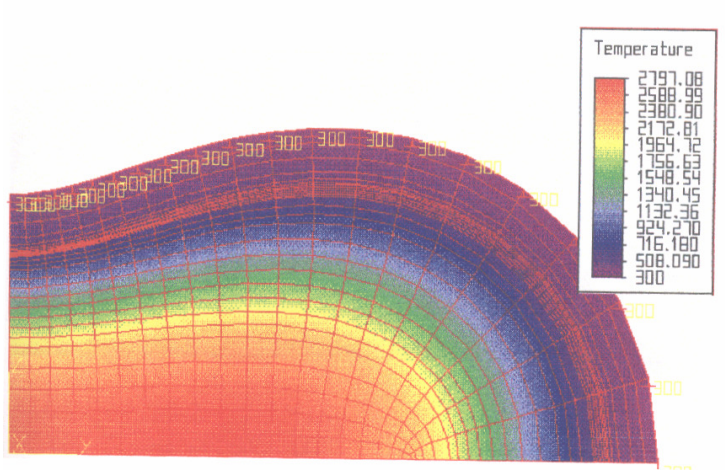

Fig. 2 Temperature distribution for the $m = 0.7$ and $v = 0.5$ format

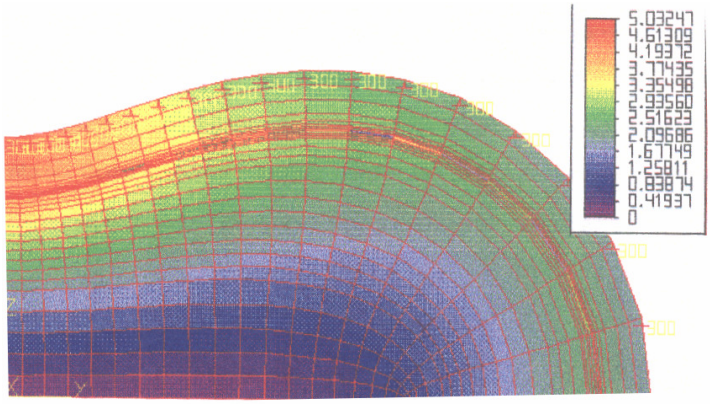

Fig. 3 Flux magnitude for the $m = 0.7$ and $v = 0.5$ format

4.2 Comparisons and Conclusions

The temperature field and the flux magnitude, as generated by the numerical procedure presented above, were compared to the results provided by the analysis of a known solution to this problem: the case of the circular rod. Local form of the energy equation, Eq. (6), in cylindrical coordinates, under permanent conduction conditions, gives:

$$Div(\mathbf{k}.\nabla\theta) + q_b = 0 \tag{25}$$

or, considered the symmetry of the problem:

$$\frac{d^2\theta}{dr^2} + \frac{1}{r}\frac{d\theta}{dr} + \frac{q_b}{k_*} = 0 \tag{26}$$

whose solution is:

$$\varphi = \varphi_0 - \frac{q_b}{4\kappa_\bullet} r^2; \quad \varphi = \frac{1}{\kappa_\bullet}\int_{\theta_\bullet}^{\theta} \kappa(\theta) d\theta; \quad \varphi = \hat{\varphi}(\theta) \quad 0 \le r \le R \tag{27}$$

where θ_* is a reference temperature, possibly $\theta^* = 0°C$, and κ_* is the corresponding core material conductivity. Values of the φ integral are tabulated results, (Tu. C.C., 1974).

For the gap region, $R \le r \le R + f$, a average conductivity may be assumed, so that continuity of heat flux makes $-k_2 \left.\frac{d\theta}{dr}\right|_{R+f} = -\frac{q_b R}{2k_1}$ and therefore:

$$\theta(r) = \theta_R - \frac{q_b R^2}{2k_2} \ln\frac{r}{R}; \quad \theta_R = \theta_{1S_2} \tag{28}$$

while for the cladding sector:

$$\theta(r) = \theta_{R+f} - \frac{q_b}{2k_3} R(R+f) \ln\frac{r}{R+f}; \quad \theta_{R+f} = \theta_{2S_3} \tag{29}$$

Set a value for the temperature of the cladding-fluid interface, $\theta_{3S_4} = \theta_f$, convection conditions will lead to $h_c = \frac{q_b R}{2(\theta_f - \theta_\infty)} \frac{R+f}{R+c+f}$ and a flux $q_f = q_b \frac{R}{2}$ that may compared to the critical flux q_{cr} for the boiling water. Corresponding results obtained under more general conditions, is shown in Fig. 6 and Fig 7, using the finite element method.

A 3D model of this problem, including fluid flow would entail a verification of the thermal coefficients used in the analysis. Here experimental values were used, as the problem was treated as 2D. Complications were caused by the boiling effect ,that PWR reactors do not have. For them, the same kind of analysis would produce very much similar temperature and flux distribution, as shown ahead.

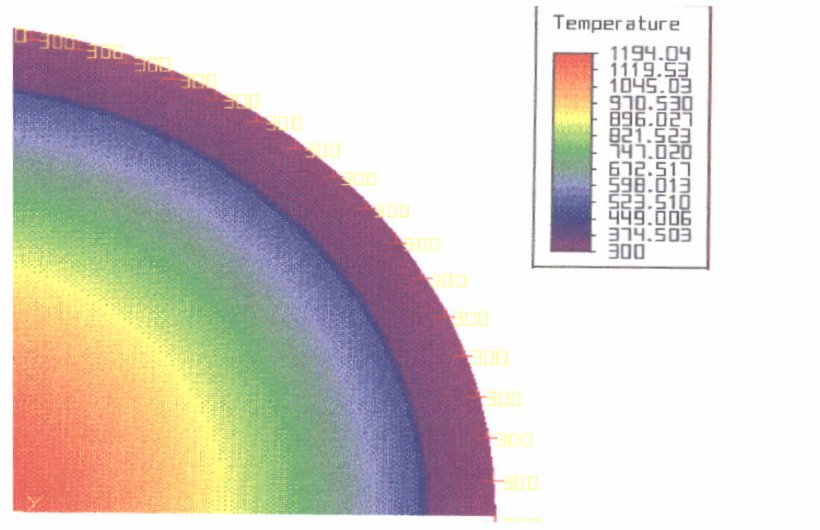

Fig. 6 Temperature distribution for the circular rod

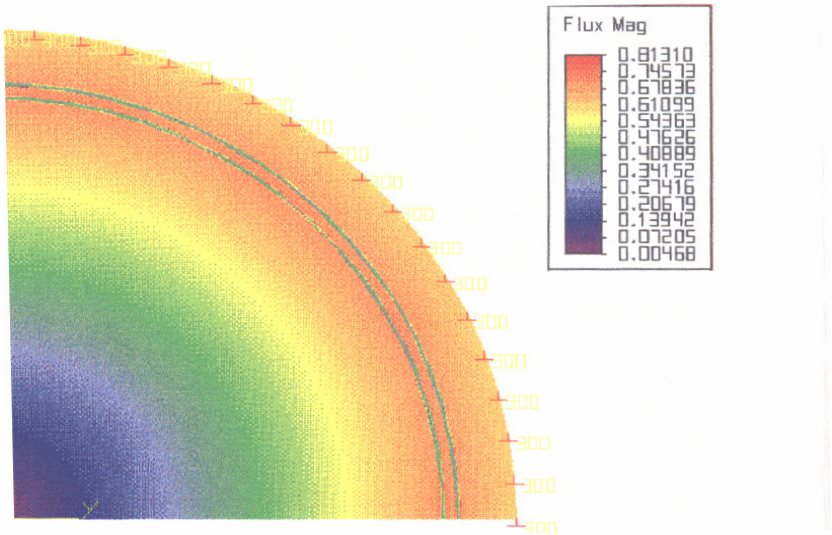

Fig. 7 Heat flux distribution for the circular rod

4.2 Optimum Form

More than 30 elements of the family of formats proposed were analyzed in what says respect to the thermal performance. Sometimes there was improving of performance, sometimes not. Thinner formats, tending to the thin plate, showed better gains. Of all cases, in BWR reactors the one corresponding to the pair $< 0.8; 0.2 >$ represented the best gain. Maximum temperature was not always the limit. In this case this occurred.

\

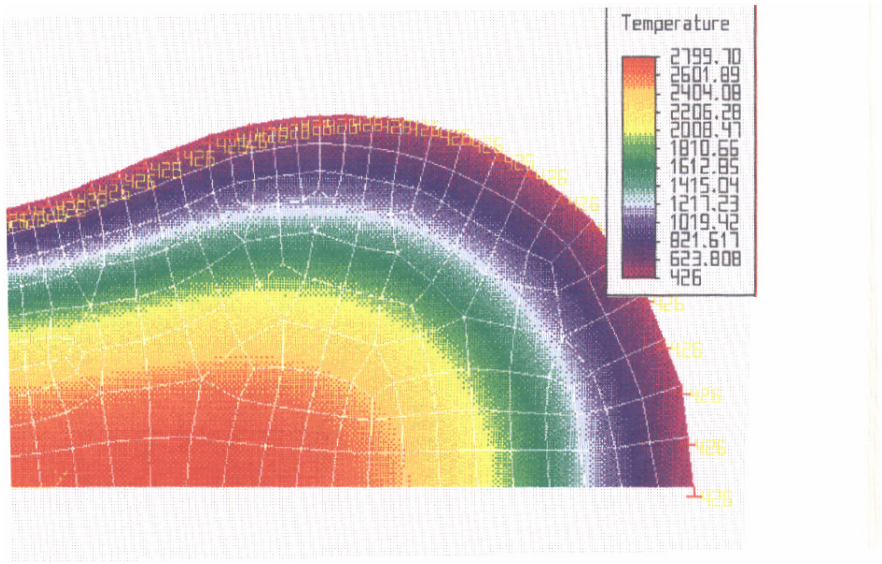

Fig. 7 Temperature distribution for the $< 0.6; 0.6 >$ format

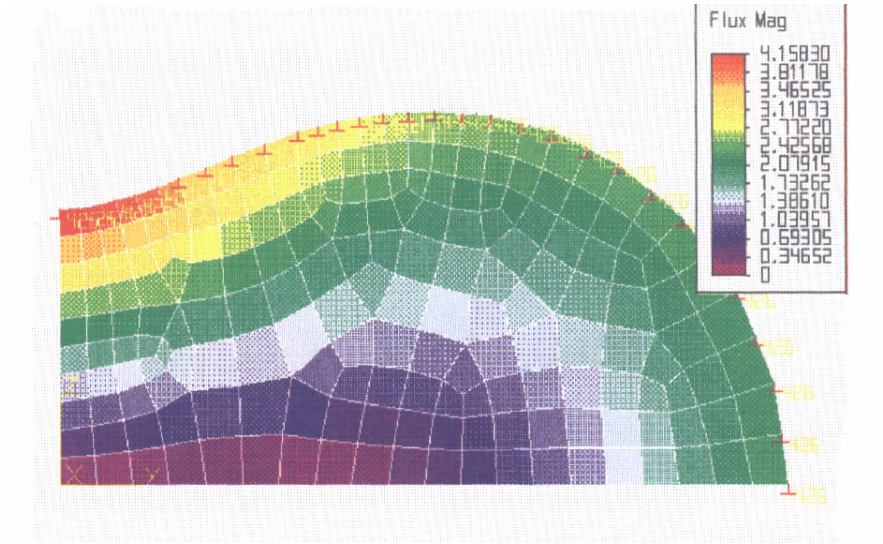

Fig. 8 Heat flux distribution for the $< 0.6; 0.6 >$ format

5. Conclusions

Flux distribution along the outer surface of the family of new formats is never constant, even when temperatures are fixed. Critical flux points, in general occurred in the thinner regions. Once obtained this point performance was measured through the q_b value. However as only the local capacity of heat transfer is exploited, additional gains could be obtained if the full capacity, corresponding to the setting of this limit to the whole surface of the element, was attained. Also use of pressurized vessels, PWR, would improve gains as the critical flux values could be increased.

6. References

Glasstone & Sesonski, **Nuclear Reactor Engineering**, Chapman & Hall, 2nd ed., 1995

Cayley, A., **An Elementary Treatise on Elliptic Functions,** Dover Publications, New York, 2nd ed.. 1961

Bathe, Klaus Jürgen, **Finite Element Procedures in Engineering Analysis**, Prentice-Hall, 2nd ed. New Jersey, 1995

Winterton, R.H.S., **Thermal Design of Nuclear Reactors,** Pergamon Int., Oxford, England, 1981

Tu. C.C., **Estudo Preliminar sobre as Vantagens de uma Barra de Combustível com Seção Transversal Semelhante à de um Glóbulo Vermelho,** Dissertação de Mestrado, E.P., USP, 1974